LIFE PREDICTION OF BOILER TUBES IN CORROSIVE ENVIRONMENTS

S. CHAUDHURI
National Metallurgical Laboratory
Jamshedpur 831 007

Abstract

Boiler tubes of coal-fired thermal power plants, subjected to prolonged exposure at elevated temperature and pressure, continue to loose their load bearing capacity due to accumulation of several damages. The corrosion damages at the inner and outer surfaces of the tubes are responsible for reduction in tube wall thickness. The microstructural damages, on the other hand, are responsbile for reduction in the high temperature strength of the material.

In this paper a case study on "Failure of a Superheater Tube of a 500 MW Boiler" has been presented to identify the major factors responsible for failure. A method was developed to estimate the maximum service temperature, the tube had experienced, from the kinetics of oxide scale growth at the tube surfaces. Considering the influences of both corrosion and microstructural damages the life of boiler tube was predicted over a range of wall thickness, thinning rate, operating temperature and pressure.

Analysis of data clearly indicated that the failure of the superheater tube had taken place mainly due to short term overheating to a temperature of about 830°C. Comparison of predicted life for several alloy steels showed that irrespective of operating temperature, stress and damage development, optimum life and resistance to creep damage could be achieved in modified 9Cr-1Mo steel followed by 2.25Cr-1Mo steel.

Introduction

Boiler tubes of coal-fired thermal power plants are subjected to prolonged exposure at elevated temperature and pressure. They are usually designed on the basis to avoid the failure of the tubes within the stipulated design life of 100,000 hours or more under the actual operating conditions during service. Selection of suitable material is thus of great importance for economical and safe operation of the plant. Over a span of more than two decades an extensive long term stress rupture test program have been conducted on a range of alloy steels to determine their rupture strength and resistance to deformation. The data generated from such tests often exhibit a large scatter of around $\pm 20\%$ of the stress lvel.[1] This corresponds to the scatter of an order of magni-

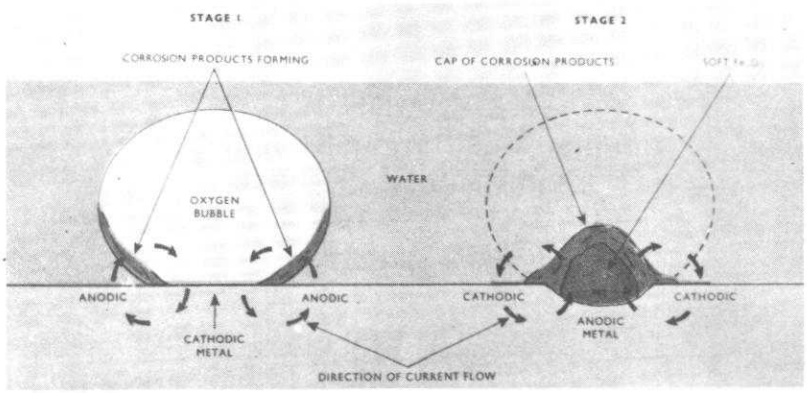

Fig. 1 : Initial and final stages of air bubble pitting

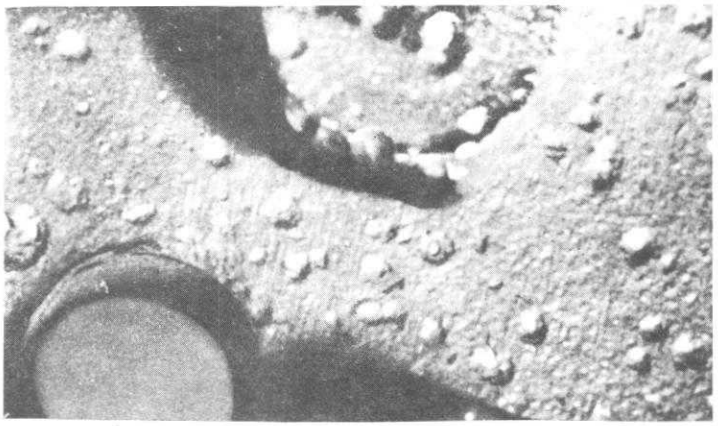

Fig. 2: Presence of air bubble pitting on the roof of a steam drum

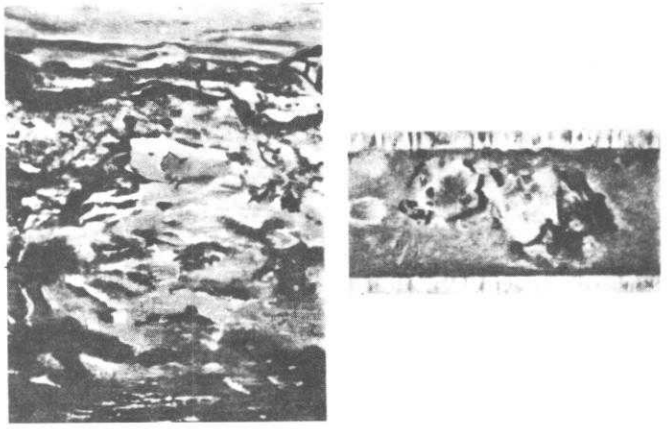

Fig. 3 : Presence of scab pitting on the water side of boiler tube surfaces

tude in the expected rupture life at any stress level. Although the design of high temperature component is based on the minimum assured level of rupture strength, a safety factor of about 1.3 to 1.6 is often used to ensure more safe and reliable operation of the plant.

In spite of such an apprehension, the failure of boiler tubes has been reported as a major cause of forced outages of boilers in coal-fired power plants. This is due to the fact that accurate prediction of life of boiler tubes is difficult because of uncertainties associated with operating conditions, material properties, erosion/corrosion rate, geometry of eroded/corroded areas etc. During continued service the load bearing capacity of the boiler time dependent damages arising from complex interaction of tubes decreases due to accumulation of tube material, operating stress and environments prevailing in the boiler. These can be broadly classified into corrosion and microstructural damages.

The corrosion damages in the form of pitting, general corrosion and scaling at the inner surfaces of the tubes are primarily responsible for reduction in the tube wall thickness. The dependence of corrosion rate and scale thickness of the tube material on the operating parameters have been described in the susequent section. The increase in operating stress due to reduction in tube wall thickness is further accelerated due to the occurence of external damaging processes viz. coal ash corrosion and fly ash erosion.

The microstructural damages, on the other hand, viz. cavitation, carbide coarsening and precipitation are responsible for reduction in the high temperature strength of the material. Microstructural studies, however, provide qualitative information on the condition of the tube material based on the understanding of microstructural changes taking place after long term exposure.

In contrast a quantitative estimate of life can be obtained from the analysis of stress rupture data using Larson-Miller Parameter.[2] The data so needed are generated experimentally from accelerated stress rupture tests. Acceleration in such tests is achieved by performing tests at higher than normal operating stress and temperature. It has been reported that whilst temperature acceleration provides a reasonable estimate of life, stress acceleration often gives an optimistic value.[3,4] The factor which could be responsible for this is that the microstructures developed in the aged material remain almost unaltered during high temperature tests. The loss of material, if any, due to significant oxidation at temperatures beyond the normal operating temperature can be minimised by performing the tests in an inert atmosphere or vacuum. The influence of wall thinning as a result of corrosion and erosion processes thus plays an important role in life assessment of boiler tubes after long term exposure. This paper highlights some observations and results on such an exercise including a case study on failure of a superheater tube of a 500 MW boiler.

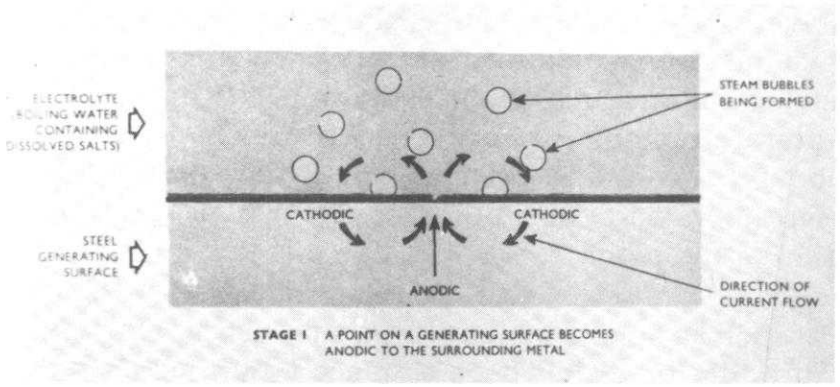

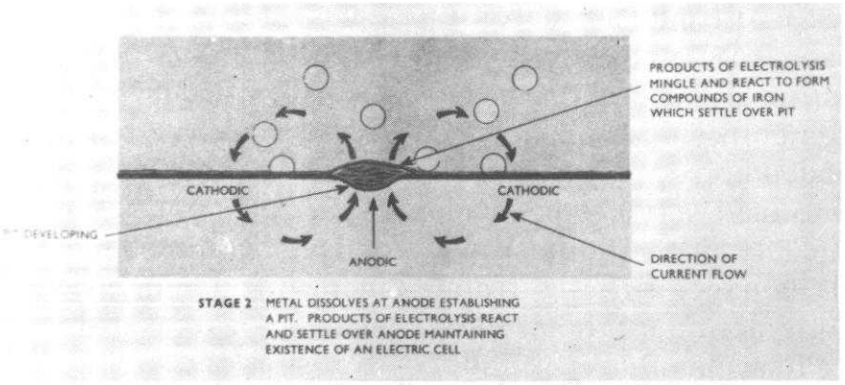

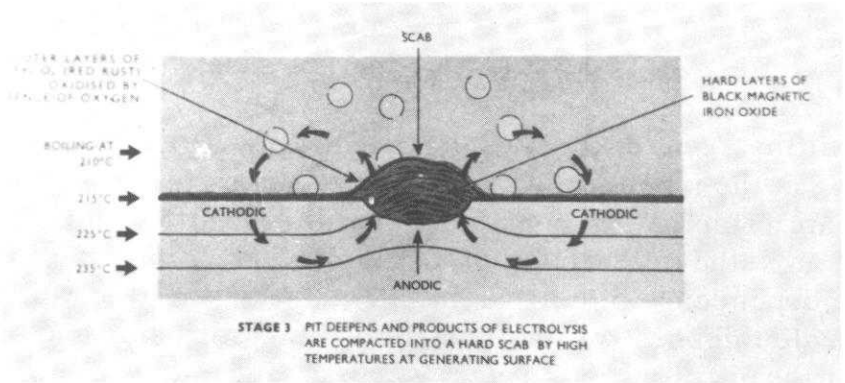

Fig. 4 : Different stages for the development of scab pitting

Pitting Corrosion

It is the worst type of corrosion often encountered on the water side of the boiler tube, mainly because of the frequency of its occurrence and its localised nature. It occurs in water having a pH value between 6 and 9. The presence of dissolved oxygen and salt in water further accelerates the corrosion rate of the tube material. The diffusion of oxygen through semi-stable protective film is responsible for occurrence of this type of corrosion. It occurs as a result of electro-chemical action, involving a difference of potential on a metal surface in which metal dissolves at the anode. The characteristics of pitting i.e., position, form, progress and the nature of the corrosion products, are strongly dependent on the conditions prevailing in the various sections of the boiler. The various types of pitting encountered in sevice may be classified into three groups:

(i) air bubble pitting;
(ii) scale pitting and
(iii) soft scale pitting.

Air bubble pitting is associated with oxygen bubbles adhering to metal surfaces. The amount of oxygen which is dissolved in water varies considerably with the temperature and pressure of the water. Depending on the operating conditions, oxygen is thrown out of solution and rises as bubbles and ultimately collects in any suitable pockets such as the tops of steam and water drums, around steam outlet etc., attaching itself to the metal surface. Electrolytic action is initiated between the oxygen rich cathodic surfaces under the bubble and the surrounding water areas which are less rich in oxygen. The products of electrolysis combine to form compounds of iron, which settle over the bubbles as a film of ferric hydroxide. This forms a semi-permeable membrane allowing the passage of ions but interferes with the ingress of oxygen. When oxygen penetrates this membrane or cap, it will be rapidly used up by the oxidation of outer layers of corrosion products before it can reach the anodic surface at the base of pit. Ultimately a stage is reached where the oxygen under the membrane is completely exhausted by the oxidation of the product of electroysis and the direction of current is reversed. Pitting continues as long as the difference in oxygen content exists.

The initial and final stages of air bubble pitting is shown in Fig. 1 and its presene on the roof of a steam drum in Fig. 2[5]. It occurs mainly when the boiler is shut down i.e., when the agitation within the boiler is nil. The corrosion products consist of an outerlayer of soft red iron oxide (Fe_2O_3) and the remainder of the pit filled with powdery black iron oxide (Fe_3O_4).

Scab pitting, however, occurs on the hot areas of generating surfaces, such as fire side of the tubes and is associated with the formation of a hard black scab of corrosion products. Its presence on the water side of boiler tube surfaces is shown in Fig. 3[5]. The conditions suitable

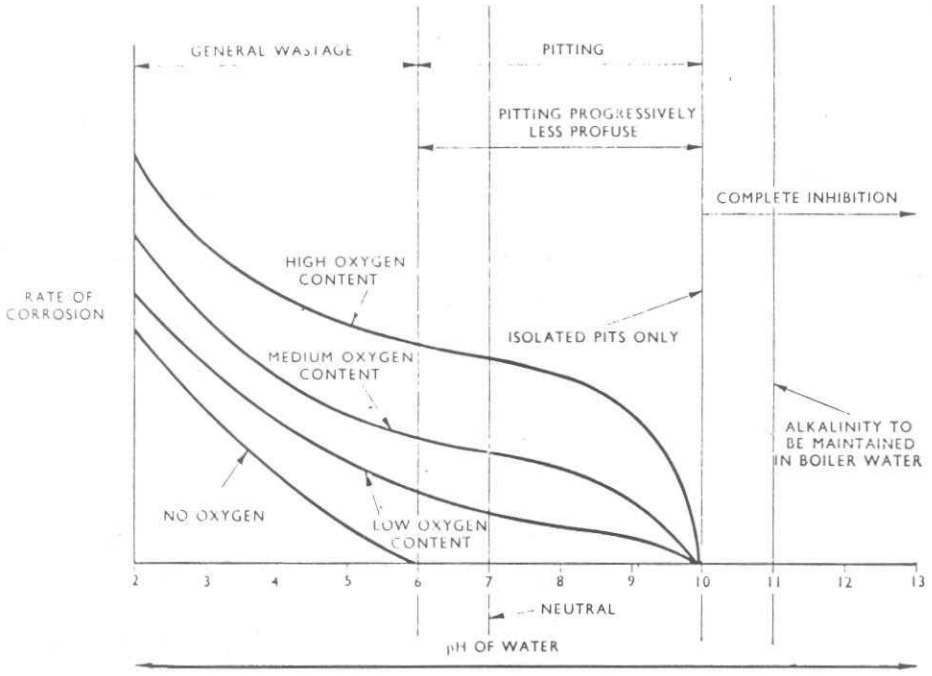

Fig. 5 : Dependence of corrosion rate of steel on oxygen content and pH of water at atmospheric temperature and pressure

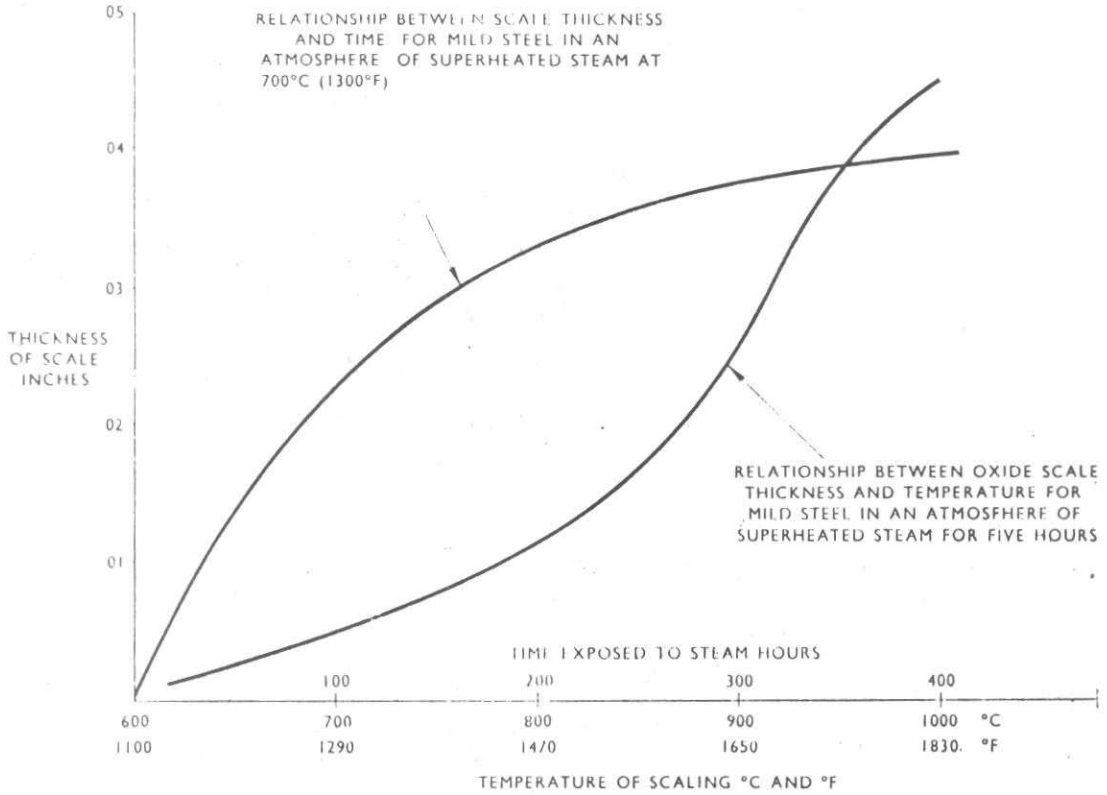

Fig. 6 : Dependence of oxide scale growth on exposure time and temperature of mild steel

for initiation of such damages on a metal surface, although not fully understood, may include the presence of oxygen bubbles, non-homogeneity of boiler materials, cracks in oxide scale, stress concentrations and local breakdown of protective films. Of these, the last one is probably most common because of the partial breakdown of the film in boiler water with a pH value ranging from 6 to 9. The different stages for the development of this type of pitting is shown in Fig. 4. The rate of attack increases with increasing temperature.

The appearance of soft pitting is similar to normal scab pitting except that the cap of corrosion product is softer and contains a high percentage of red iron oxide (Fe_2O_3). It occurs mainly in superheater tubes, headers, and main steam pipes. When the boiler is shut down, condensation will result in droplets of moisture being formed on the metal surfaces which will then dissolve the deposited salts and produce small droplets of fairly concentrated electrolyte. A stage, similar to the formation of air bubble pitting, is thus reached in which anodic attack proceeds in areas less rich in oxygen.

General Corrosion

In contrast to pitting corrosion, general corrosion is of a more uniform nature rather than a selective attack. It implles the reduction in metal thickness over comparatively large areas in a fairly uniform manner. Thinning of tube wall water surfaces in which the thickness of the metal is gradually reduced by corrosion is an example of this type of corrosion.

Corrosion of steel in acid solution proceeds in an even and non-selective manner owing to the non-development of protective films of corrosion products. It is evident from Fig. 5 that the rate of corrosion is strongly dependent on the amount of dissolved oxygen and pH value of water. When pH is below 6, corrosion proceeds rapidly even without the presence of oxygen and occurs when metal dissolves in acids to liberate hydrogen e.g.,

$$Fe + 2HCl = FeCl_2 + H_2$$

The rate at which metal dissolves depends on the strength and temperature of the acid and nature of the surface being dissolved. The presence of oxygen further accelerates the rate and range of general corrosion. The concentration of slats dissolved in solution degree of dissolved oxygen and the temperature involved influence the rate of attack. Corrosion, however, could be inhibited when a rise in alkalinity above a definite value promotes the formation of stable protective film.

High Temperature Oxidation

Various types of corrosion as described in the preceeding sections are a form of oxidation, since iron is converted into its oxides when corrosion takes place. The term oxidation is, however, used in a more

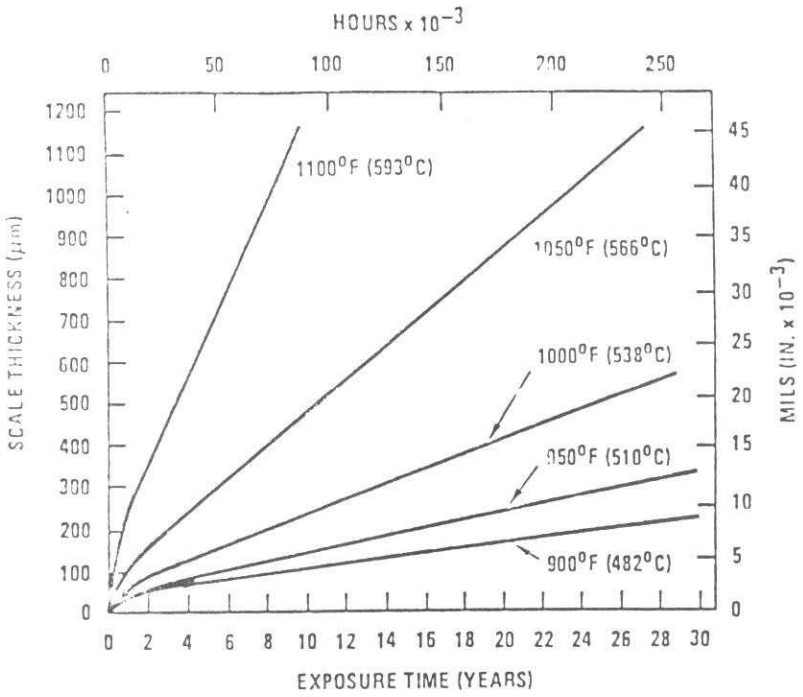

Fig. 7 : Dependence of oxide scale growth on exposure time and temperature of 2.25Cr-1Mo steel

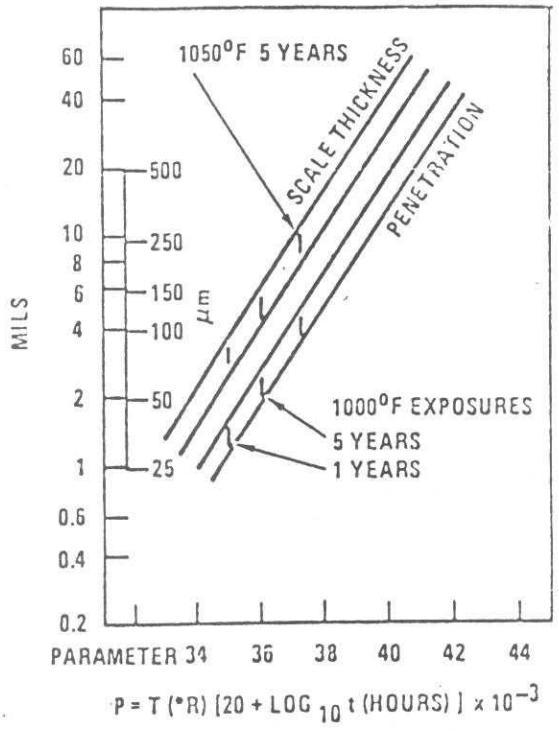

Fig. 8 : Parametric representation of oxide scale growth of 2.25Cr-1Mo steel

restricted sense refering to direct reaction between gaseous oxygen and iron. The problem becomes serious above 550°C and hence described as high temperature oxdiation. The reaction which takes place when iron is heated in a current of steam is

$$3Fe + 4H_2O = Fe_3O_4 + 4H_2$$

A hard black magnetic iron oxide (Fe_3O_4) scale is thus formed over the metal surfaces. The rate at which this scale is formed depends on several factors viz metal temperature, exposure time at this temperature and the rate at which overheated metal is supplied with a fresh oxidising atmosphere. The dependence of oxide scale growth on these factors for mild steel are shown in Fig.6.[5] Similar nature of dependence in case of 2.25Cr-1Mo steel, as reported in literature are also shown in Fig. 7[6,7]. From these figures it would be possible to generate data on oxide scale thickness as a function of time-temperature parameters viz. Larson-Miller Parameter (LMP) so as to construct a master rupture plot (Scale thickness vs. LMP plot). A typical such plot for 2.25Cr-1Mo steel is shown in Fig. 8[8]. From the knowledge of scale thickness produced at the boiler tube surfaces, one can estimate the required time-temperature parameter from this plot. This helps further in estimating the temperature, the tube had experienced, simply by substituting the exposure time of the tube in time-temperature parameter. For a better understanding of the importance and application of this approach for estimation of tube wall temperature, a case study on "Failure of a superheater tube of a 500 MW boiler"[9] has been presented in the proceeding section. This was chosen mainly because the failure of tubes by overheating and scaling is often encountered in service. Such scaling at the tube wall may result in a sudden failure by bursting, continued thinning to perforation and local bulging of any tube. Factors governing such failure include general water starvation, thick layer of insulting scale build up and/or defective circulation.

Failure of Superheater Tubes - A case study

Background

Failure of superheater tubes of a 500 MW boiler occured during trial run following a service exposure of about 100 hours. Material specification and operating parameters of the tubes are summerised in Table-I.

Table - I
Material Specification & Operating Parameters of Superheater Tubes

Material	:	2.25Cr-1Mo Steel as per ASTM A213 T22
Outer diameter	:	44.5 mm
Thickness	:	10 mm
Steam temp.	:	560°C-580°C
Steam Pressure	:	185kg/cm^2
Steam flow rate	:	1700tons/hr

The tube samples selected for this investigation, as shown in Fig.9,are (i) a piece of tube from the zone of

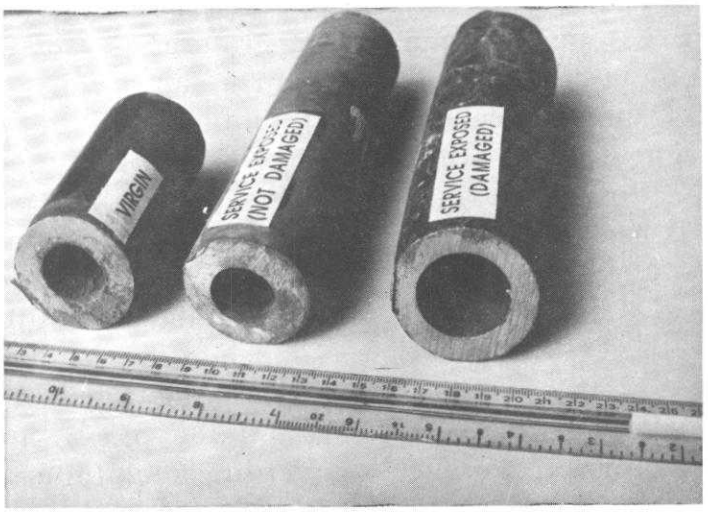

Fig. 9 : As received superheater tube (a) failed; (b) adjacent to failed and (c) virgin

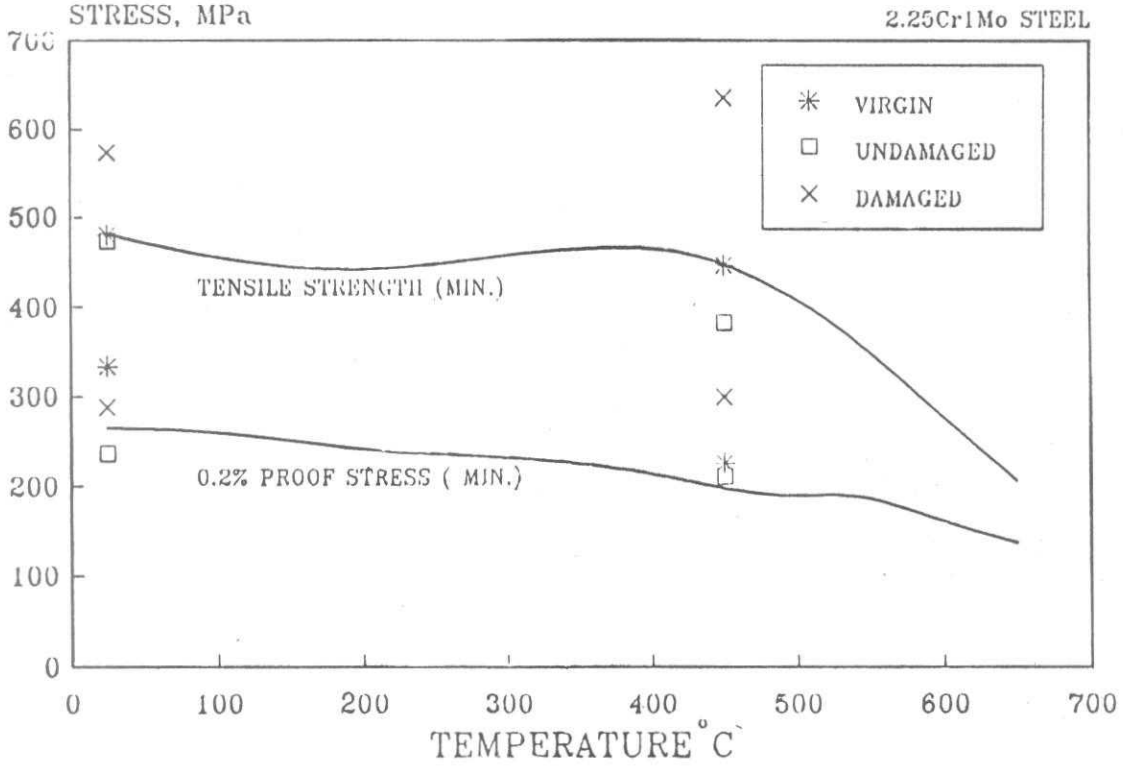

Fig. 10 :Tensile properties of as received tube samples compared with minimum specified properties of 2.25Cr-1Mo steel

failure;
(ii) a piece of tube adjacent to the failed tube and
(iii) a piece of virgin tube.

In order to identify the main cause of failure, the detailed investigation viz. chemical analysis, hardness measurement, evaluation of tensile properties and microstructural study have been carried out.

Results and Discussion

The chemical composition of the failed and virgin tube, reported in Table - II, indicates that the chemistry of both tubes meets the ASTM specification.

The outer diameter of the failed tube was found to be 49.2 mm against the original diameter of 44.5 mm. The most significant point in this case is the gross circumferential expansion of the failed tube upto about 19%. Such extensive expansion connot be expected under normal operating condition within a short span of service exposure of about 100 hours.

It is evident from the measurement of hardness at the inner surface, mid section and outer surface of all tubes (Table - III) that the hardness of the failed tube is significantly higher than that of virgin and undamaged tubes.

Table - II
Chemical Composion (inWt%)

Element	Failed Tube	Virgin Tube	Specification ASTM A 213 T22
Carbon	0.12	0.1	0.06-0.15
Manganese	0.41	0.42	0.30-0.60
Silicon	0.22	0.22	0.50 max
Phosphorus	0.013	0.012	0.025 max
Sulphur	0.003	0.003	0.025 max
Chromium	2.16	2.13	1.90-2.50
Molybdenum	1.05	1.00	0.87-1.13

Table - III
Hardness Values of as Received Tubes

Tubes	Hardness, HV2O		
	Inner	Middle	Outer
Virgin	145	149	151
Undamaged	143	143	145
Failed	179	178	180

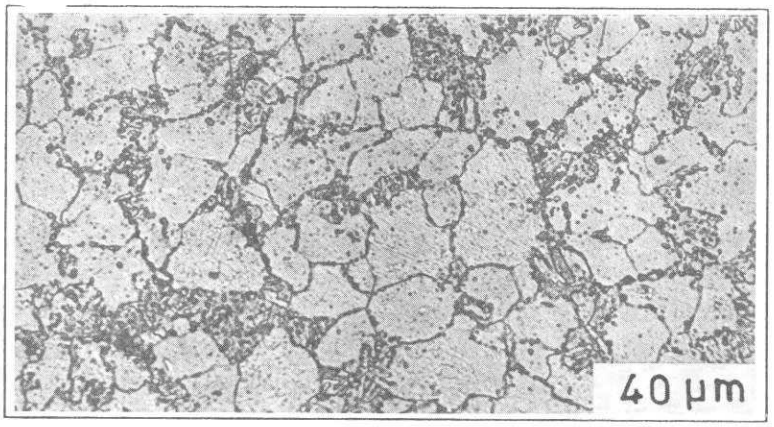

Fig. 11: Microstructure of virgin tube consisting of ferrite and tempered bainite.

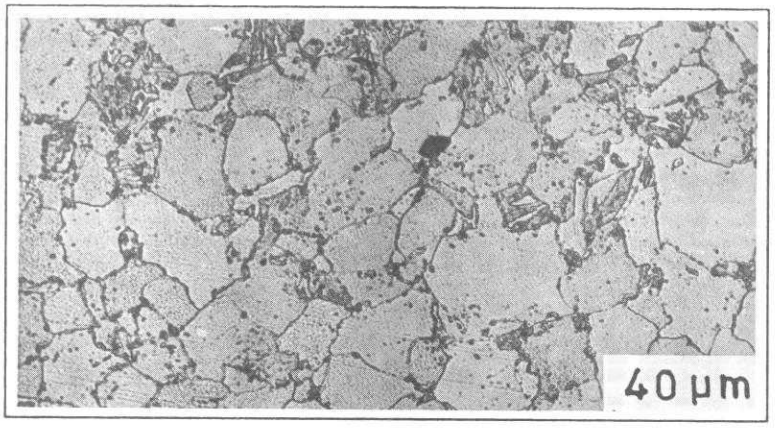

Fig. 12 : Microstructure of undamaged tube consisting of ferrite and tempered bainite.

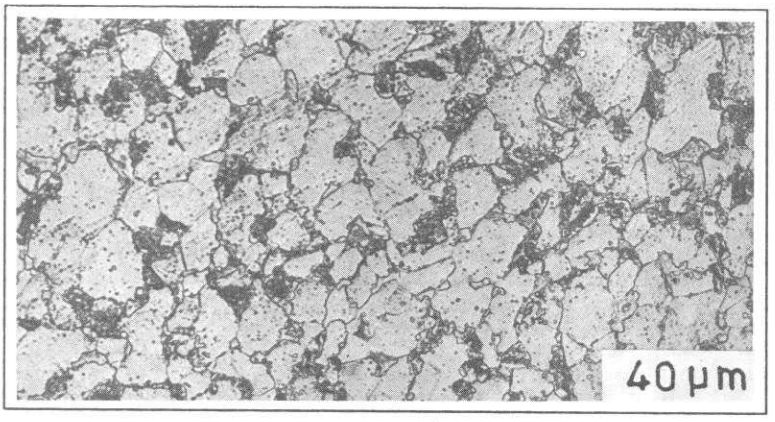

Fig. 13 : Microstructure of failed tube showing freshly formed bainitic areas.

The tensile properties of all tubes, as shown in Fig. 10, revealed that irrespective of test temperature all the tubes meet the minimum specified properties of 2.25Cr-1Mo steel. The tensile strength of the failed tube is, however, significantly higher than that of the other tubes.

The microstructures of virgin (Fig. 11) and undamaged (Fig. 12) tubes are almost similar, consisting of ferrite and tempered bainite. In contrast the microstructure of the failed tube (Fig. 13) showed the presence of freshly formed bainitic areas. Besides the oxide scale thickness on the inner surface of the failed tube Fig. 14 was found to be several folds more than that of the undamaged tube (Fig. 15). In the failed tube the oxide scale thickness was of the order of 0.25 mm.

All the above observations can be reconciled in a situation only if the temperature had exceeded the lower critical temperature which is reported to be about 800°C for 2.25Cr-1Mo steel.

In order to predict the extent of temperature excursion beyond the critical temperature some detailed analysis was made based on oxide thickness as obtained on the inner surface of the failed tube. Published kinetic data on oxide scale growth of 2.25Cr-1Mo steel[10] have been used for this purpose. The predicted time-temperature profiles for a range of service exposure to develop 0.25 mm thick oxide at the inner surface of the failed tube are shown in Fig. 16. Since the presence of freshly formed bainite is an indicative of temperature excursion beyond the lower critical temperature, the most probable profile that the tube experienced is the one having an exposure of 2 hours, the maximum temperature being 830°C. Corresponding to each time-temperature profile (Fig. 16), accumulation of strain and the diametrical expansion of the tube have been calculated and presented in (Fig. 17). The creep strain predicted from the time temperature profile for 2 hours exposure comes to about 1% which is indeed quite lower than the observed value of 19%. It is mainly because the existing material database in the temperature range of 500°C to 600°C has been used for extrapolation. Clearly there is a need to collect creep data at temperatures beyond 600°C.

In order to ensure whether it is possible to achieve a creep strain of about 19% within a short time at 830°C, a short term creep test has been carried out in the laboratory. Based on this it has been established that a creep strain of about 16% is achievable in less than 2 hours at 830°C and at a stress level of 30 MPa which represents the hoop stress corresponding to the maximum operating pressure of 185 kg/cm^2 for the tube in question. This, therefore, conclusively proves that the failure of the tube took place due to short term overheating to a temperature of about 830°C. Partial chocking of the tube by some foreign material could be responsible for such overheating. The other tubes, however, did not suffer any heavy

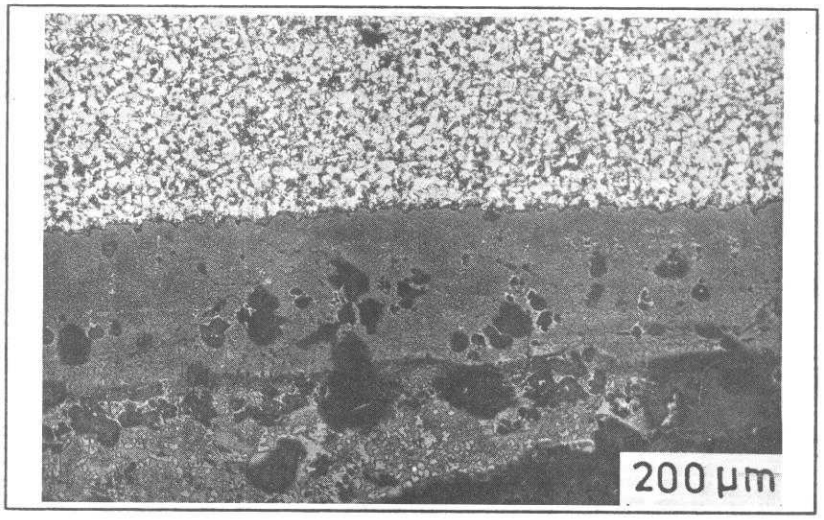

Fig. 14 : 0.25 mm thick oxide scale at inner surface of failed tube

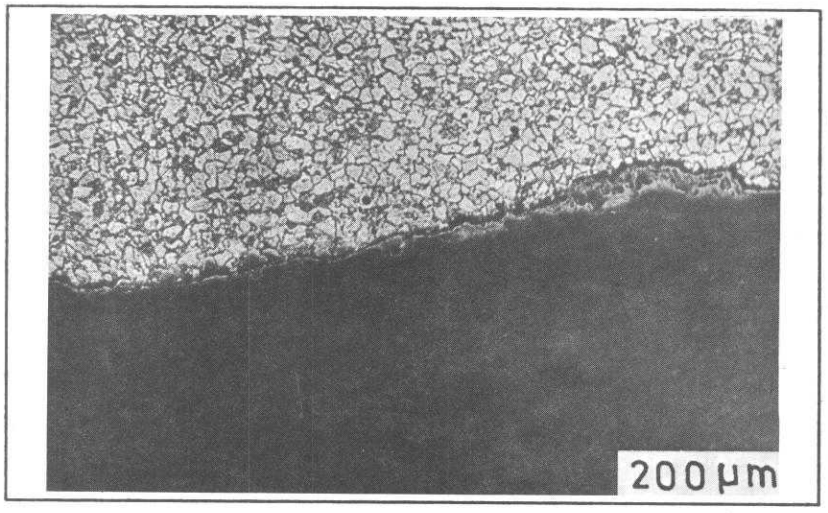

Fig. 15 : Insignificant oxide scale at inner surface of undamaged tube

temperature excursion beyond 650°C.

Although the high temperature mechanical properties of service exposed components are often found to be better than the minimum specified level, the component dimensions often change as a result of prolonged service. The most prominent amongst these is the loss of tube wall thickness. The growth of oxide scale at tube surfaces is primarily responsible for this. Other external processes such as coal ash corrosion, flame impingement and fly ash erosion also contribute to such damage development in service. A need is thus felt to look into the life prediction problems considering the influence of wall thinning due to the existence of corrosion and erosion processes during operation of the plant. Keeping this in view the methodology recently developed for creep life estimation of boiler tubes under wall thinning condition has been described in the next section.

Life Estimation Under Wall Thinning Condition

Method of life estimation

A simple method for estimating creep life of boiler tubes in presence of corrosion and erosion processes has recently been proposed by Zarrabi.[11] This is based on calculation of reference stress for the tube as a function of time assuming constant thinning rate on either side of the tube. For various components, expressions for reference stress are available in the literature.[12] Such an expression for boiler tube is given by

$$\sigma_{Ref} = (\sqrt{3}/2) .k.Pe/\ln[(d+H)/(d-H)] \quad (1)$$

where Pe is the effective operating pressure, d is the mean diameter, H is the wall thickness at any time t and K is a constant describing the nature of wall thinning i.e., whether the thinning is uniform and/or localised. In case of uniform thinning K becomes equal to one. One can, however, estimate life under wall thinning condition based on calculation of hoop's stress for the tube as a function of time. Expression for hoop's stress is given by

$$\sigma_{Hoop} = Pe.d/(2H) \quad (2)$$

For a constant thinning rate (H^o), wall thickness atny time (t) can be expressed as

$$H + H_o - H^o. t \quad (3)$$

where Ho is the initial wall thickness of the tube. Another important factor to be considered for life estimation is the prediction of stress rupture properties of service exposed material from its master rupture plot. The intersection of two curves representing σ_{Ref} or $\sigma_{Hoop} = f(t)$ and σ rupture $= g(T,t)$ provides an estimate of life, where $\sigma_{rupture}$ is the time dependent rupture strength at a temperature (T).

Some observations and results on estimated creep lives of several alloy steels[13-18] over a wide range of operating temperature, pressure,

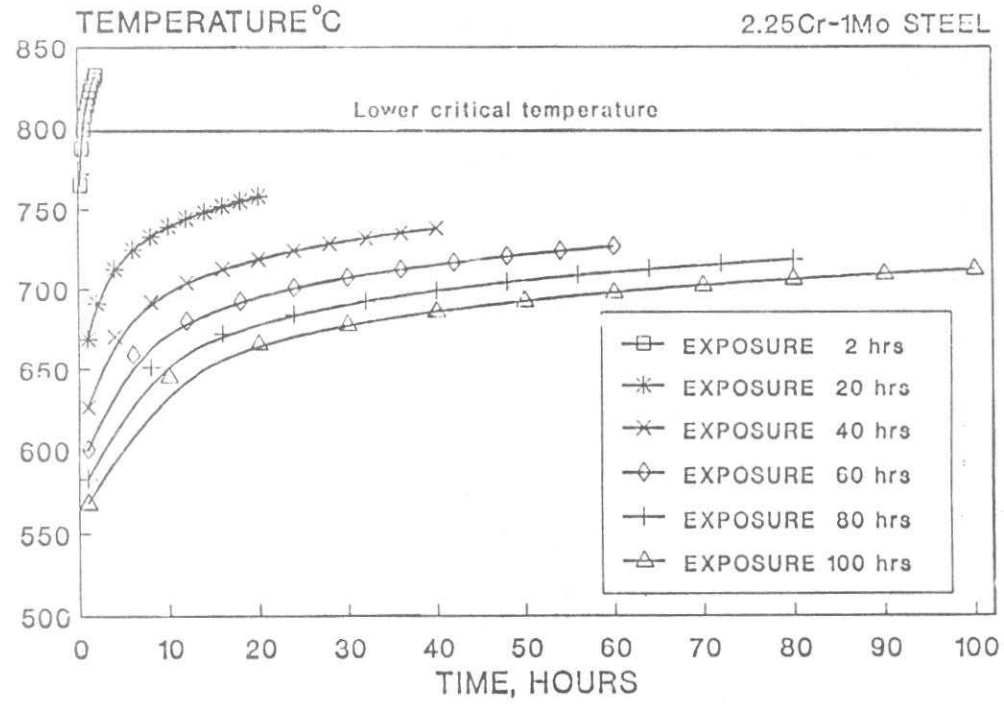

Fig. 16 : Predicted time temperature profiles to develop 0.25 mm thick oxide scale at inner surface of the failed tube

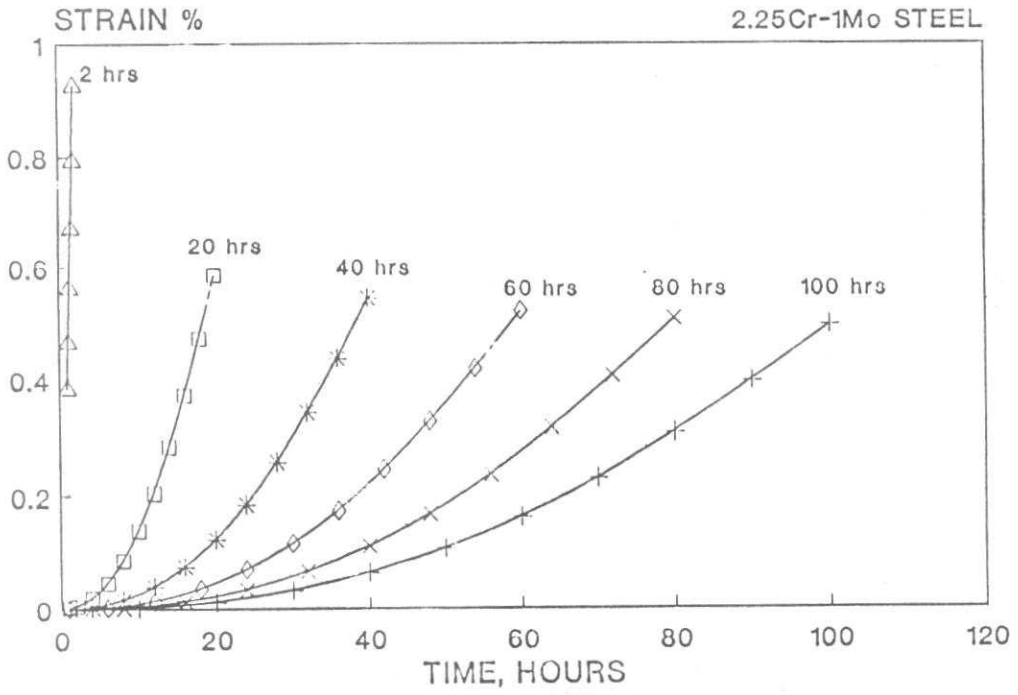

Fig. 17 : Predicted creep strain corresponding to time temperature profiles shown in Fig. 16.

tube wall thickness and thinning rate are presented and discussed in the following section. The material database and the range of parameters selected for this study are summarised in Table - IV and Table - V respectively.

Table - IV
Materials Database

0.50Cr - 0.5Mo Steel [13]
1.00Cr - 0.5Mo Steel [14]
5.00Cr - 0.5Mo Steel [15]
2.25Cr - 1.0Mo Steel [16]
9.00Cr - 1.0Mo Steel [17]
Modified 9Cr Mo Steel [18]

Table - V
Parameters Selected

Temperature°C	:	535-600
Pressure, MPa	:	10-18
Original Tube wall thickness, mm	:	5-10mm
Thinning rate, mm/year	:	0.22-0.75
Original outer diameter, mm	:	50

A sample procedure to illustrate how to predict the influence of initial wall thickness on creep life of boiler tubes[16], based on this approach are described below:

(a) Compute σ_{Ref} as a function of life for constant operating pressure and thinning rate of the boiler tube using equations (1) and (3).Repeat this procedure for a wide range of initial wall thickness of the tube. Display the results graphically i.e., $\sigma_{Ref} = f(t)$ (Fig.18).

(b) Analyse stress rupture data of the service exposed material using Larson-Miller Parameter to construct a master rupter plot. Such a plot can be represented by a polynomial equation:

$$LMP = T(20 + \log tr) = a_o + a_1 \log\sigma + a_2 (\log\sigma)^2 + \ldots + a_m(\log\sigma)^m \quad (4)$$

where T(°K) is temperature, σ(MPa) is stress, tr(hrs) is rupture time and a_0, a_1, a_2, . . ., am are correlation coefficients evaluated from least squar analysis of stress rupture data. Estimate stress rupture properties at given temperature (e.g., 575°C, 600°C) from equation (4). Superimpose stress rupture curves on the curves represening $\sigma_{ref} = f(t)$(Fig. 18)

(c) Compute life from the intersection of the curves represented by equations (1) and (4).

(d) Repeat the steps (a) to (c) to predict creep life of other materials[13-18] considering the influences of several parameters such ash thinning rate, operating temperature and pressure.

Following this procedure the creep lives have been predicted for several grades of boiler tube materials over a wide range of parameters as given in Table - V.

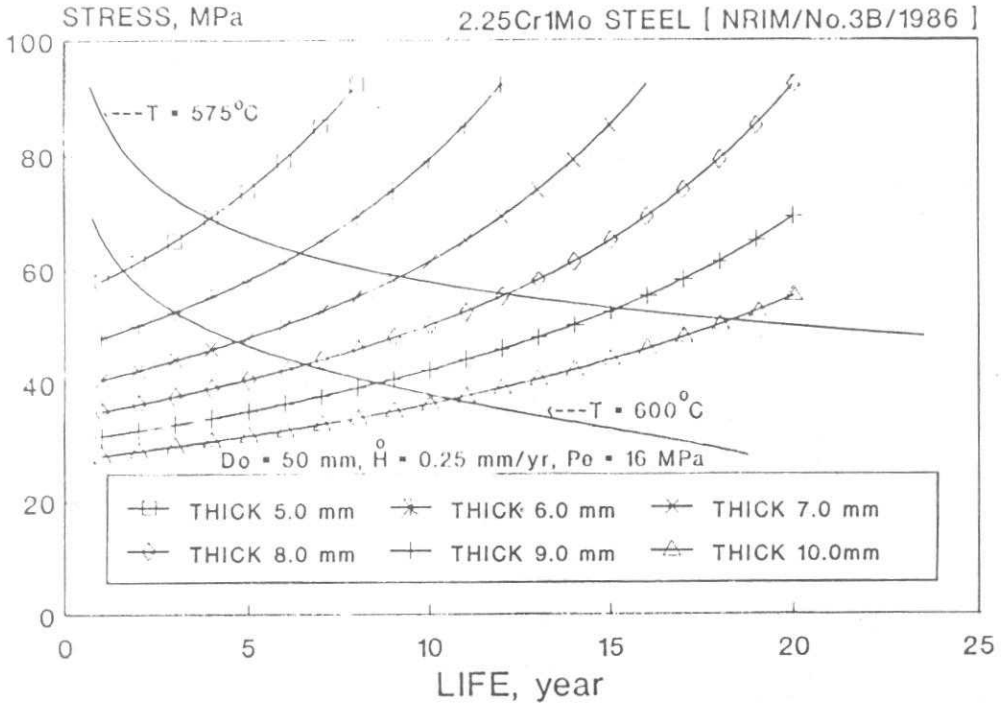

Fig. 18 :Method describing creep life prediction of 2.25Cr-1Mo steel at 575°C and 600°C over a range of tube wall thickness

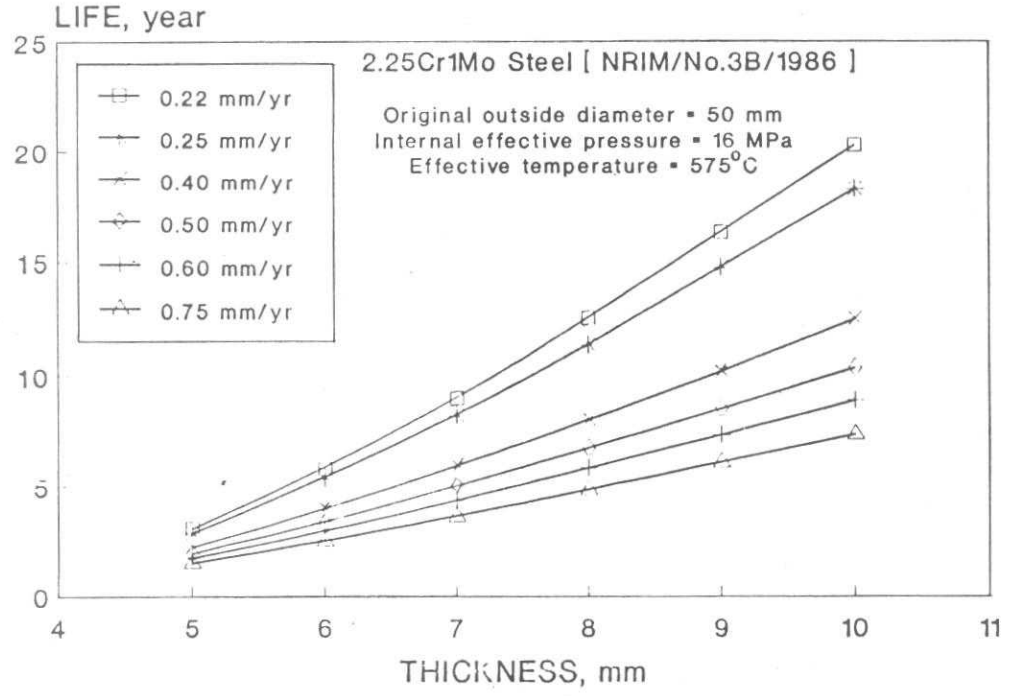

Fig. 19 : Influence of tube wall thickness and thinning rate on predicted creep life of 2.25Cr-1Mo steel

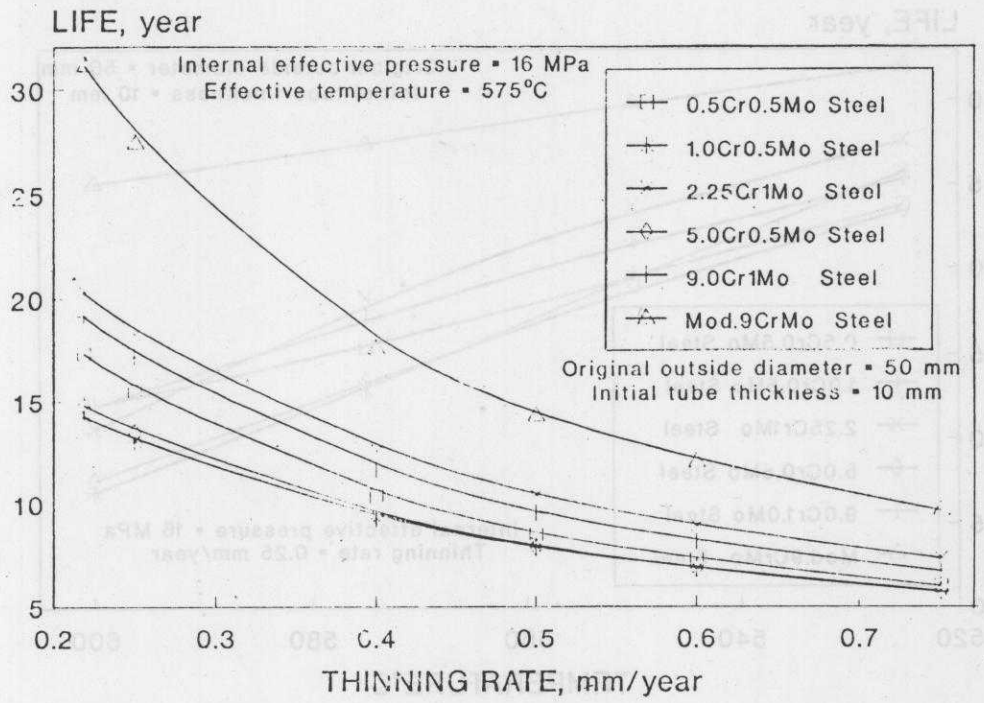

Fig. 20 :Influence of wall thinning rate on creep lives of several alloy steels

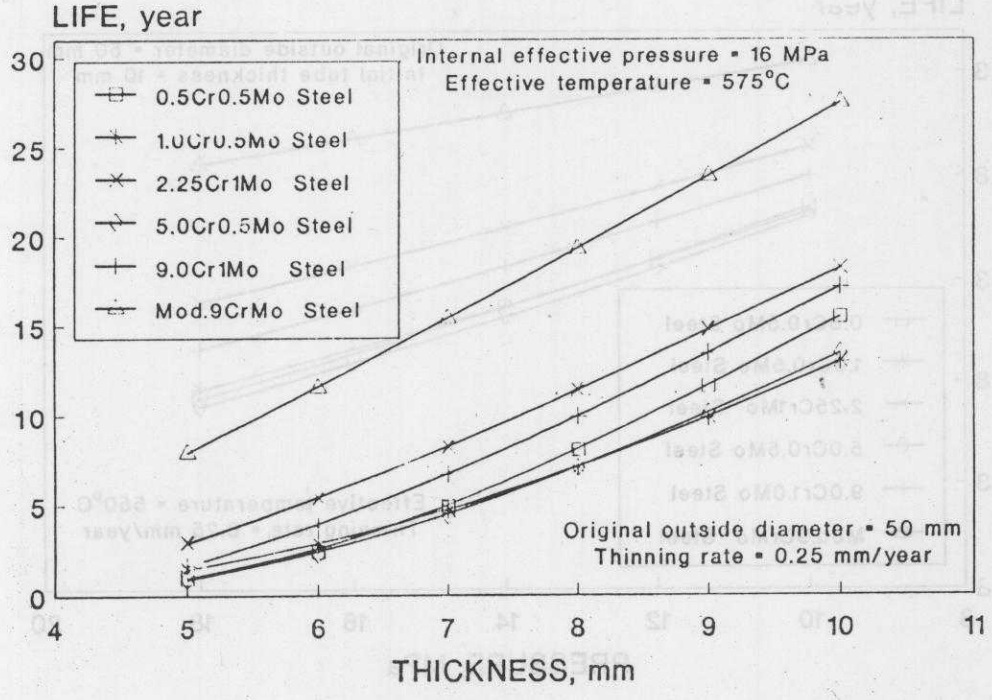

Fig. 21 : Influence of tube wall thickness on creep lives of several alloy steels

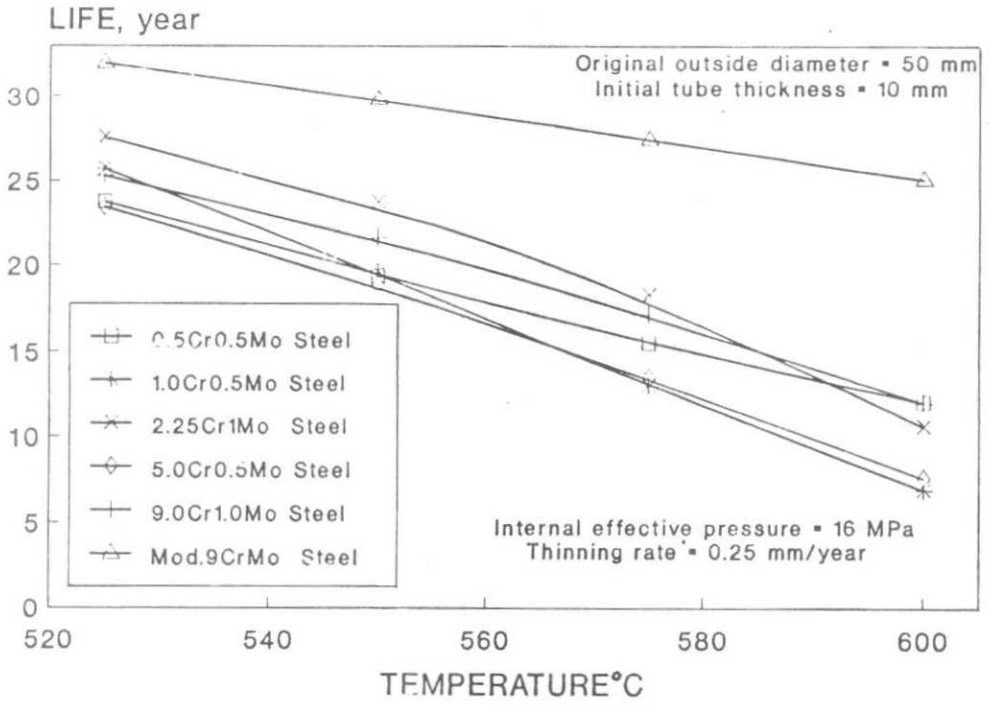

Fig. 22 : Influence of operating temperature on creep lives of several alloy steels

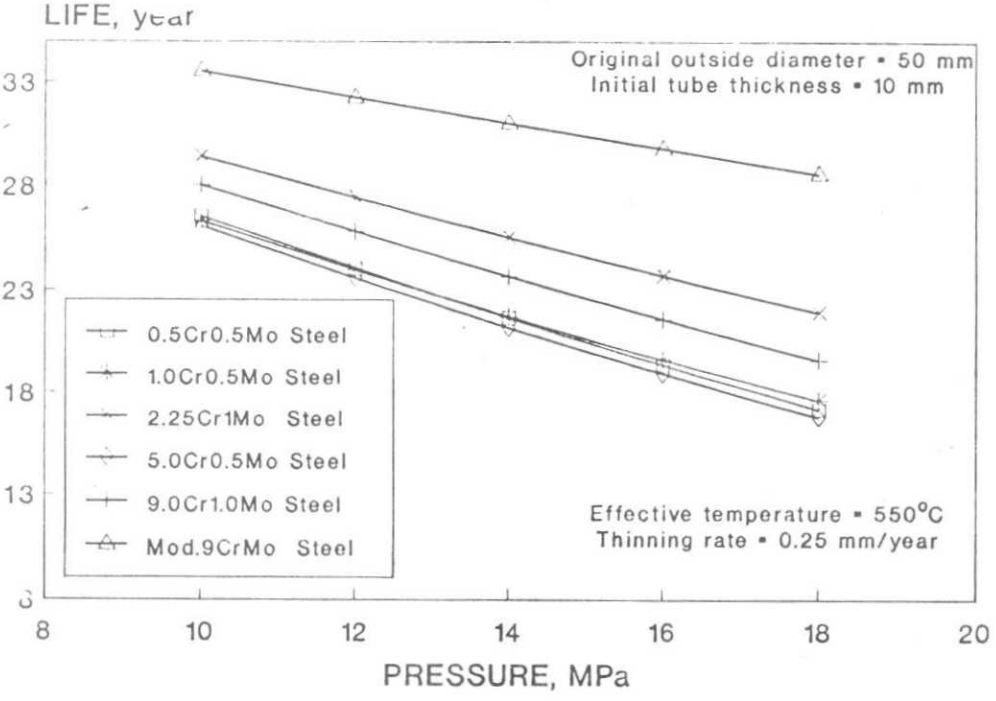

Fig. 23 : Influence of operating pressure on creep lives of several alloy steels

Results and Discussion

Influences of tube wall thickness and thinning rate on the predicted creep lives of 2.25Cr-1Mo steel, as shown in Fig. 19, reveal that (i) irrespective of thinning rate, creep life increases with increasing wall thickness; (ii) irrespective of wall thickness, creep life decreases with increasing thinning rate. As a result maximum creep life is achievable in a tube having thickest section but experienced least thinning. This is a general phenomenon observed in other grades of tube material as well.

Comparative study showed that for a wide range of thinning rate, the longest life and resistance to creep damage is achievable in modified 9Cr-1Mo steel, followed by 2.25Cr-1Mo steel, 9Cr-1Mo steel and 0.5Cr-0.5Mo steel (Fig. 20). Influence of tube wall thickness on predicted creep life (Fig. 21) also showed similar features. Influence of operating temperature (Fig. 22), however, indicated that the longest life and resistance to creep damage at all temperatures is achievable only in case of modified 9Cr-1Mo steel. Amongst other grades of steels, 2.25Cr-1Mo steel has a longer life than that of 9Cr-1Mo steel upto about 585°C, beyond which 9Cr-1Mo steel has a longer life. At a constant operating temperature of 550°C as well as for a wide range of operating pressure, modified 9Cr-1Mo steel was found to exhibit the longest life and resistance to creep damage followed by other materials, in order of decreasing life/resistance to damage, viz. 2.25Cr-1Mo steel, 9Cr-1Mo steel and 0.5Mo steels (Fig. 23).

Conclusion

In conclusion it may, therefore, be said that irrespective of operating temperature and pressure to which the boiler tubes are exposed as well as loss of wall thickness due to the corrosion/oxidation and erosion processes in service, modified 9Cr-1Mo steel exhibited the longest life/resistance to creep damage. The next candidate material recommended for such operating condition is 2.25Cr-1Mo steel upto a temperature of about 585°C, beyond which 9Cr-1Mo steel shows longer creep life.

References

1. Evans, R.W. and Wilshire, B., "Creep of Metals and Alloys", Inst. of Metals, London, (1985).

2. Larson, F.R and Miller, J., "A Time-temperature Relationship for Rupture and Creep Stresses,", Trans. ASME, 74 (1952), pp.765.

3. Wiegand, H., Granachar, J. and Sander, M., "Arch. Eisenhutenwesen", 45(1975), pp.533-539.

4. Hart. R.V., Met. Tech., 13, (1976), pp.1.

5. Boiler Corrosion and Water Treatment, Ministry of Defence, (1970).

6. Viswanathan, R., Fonlds, J.R and Robberts, D.A. "Proceedings of

the Intl. Conf. on Life Extension & Assessment", The Hauge, Inne., (1988).

7. Roberts, D.I., G.A. Technologies, San Diego, (1986).

8. Paterson, S.R. and Rettig, T.W., "Project RP-2235-5, Final Report, EPRI, 91987).

9. Chandhuri, S., Sinha, R.K., Singh, R & Ghosh, R.N., "Investigation on Failure of Final Superheaters Tubes of a 500MW boiler", NML Report, Dec. (1993).

10. Viswanathan, R., "Damage Mecanisms & Life Assessment of High Temperature Components", ASM Intl., (1989), pp.229.

11. Zavrabi, K., Int.l Jr. of Pressure Vessels & Piping, 53(1993), p.p.351-358.

12. Boyle, J.T. and Spence, J., "Stress Analysis for Creep" London, (1983), pp.119.

13. NRIM Data Sheets for 0.5Cr-0.5Mo Steel, No. 20A, (1981).

14. NRIM Data Sheets for 1Cr-0.5Mo Steel, No. 1A, (1976).

15. NRIM Data Sheets for 5Cr-0.5Mo Steel, No. 12B, (1992).

16. NRIM Data Sheets for 2.25Cr-1Mo Steel, No. 3B, (1986).

17. NRIM Data Sheets for 9Cr-1Mo Steel, No. 19, (1975).

18. Iseda, A., Kubota, M., Hayase, Y., Yamamoto, S and Yoshikawa, K., "Sumitomo Search", No. 36, May, (1988), pp.17-30.